THE SEA: THE CURRENT AND FUTURE OCEAN
Journal of Marine Research, 77, Supplement, 169–189, 2019

N-loss stoichiometry in a Peru ODZ eddy

by Mark A. Altabet[1,2] and Annie Bourbonnais[1,3]

ABSTRACT

Assuming heterotrophic denitrification as the dominant microbial process, Richards (1965) formulated a stoichiometry governing nitrogen loss in open-ocean oxygen deficient zones (ODZs). It prescribes the quantitative coupling between the oxidation of organic matter by NO_3^- in the absence of O_2 and the corresponding production of CO_2, N_2, and PO_4^{-3}. Applied globally, this relationship defines key linkages between the C, N, and P cycles. However, the validity of Richards's stoichiometry is challenged by recognition of complex microbial N processing in ODZs including anammox as an important pathway and nitrite reoxidation. Whereas Richards's stoichiometry would result in N_2-N production to NO_3^- removal rates of 1.17, dominance by anammox with respect to biogenic N_2 production could in theory result in a ratio as high as 2. Ratios with PO_4^{-3} production provide an additional constraint on the quantity and composition of respired organic matter. Here we use a mesoscale eddy with extreme N-loss in the Peru ODZ as a "natural laboratory" to examine N-loss stoichiometry. Its intense biogeochemical signatures, relatively well-defined timescales, and simplified hydrography allowed for the development of strong co-occurring gradients in NO_3^-, NO_2^-, biogenic N_2, and PO_4^{-3}. The production of biogenic N_2 as compared with the removal of NO_3^- (analyzed either directly or as N deficits) was slightly less than predicted by Richards's stoichiometry and did not at all support any "excess" biogenic N_2. PO_4^{-3} production, however, was twice the expectation from Richards's stoichiometry suggesting that respired organic matter was P-rich as compared with C:N:P Redfield composition. These results suggest major gaps remain between current understanding of microbial N pathways in ODZs and their net biogeochemical output.

Keywords: Nitrogen, oxygen, isotope, biogeochemistry, mesoscale eddy, stoichiometry

1. Introduction

In the subsurface cores of oxygen deficient zones (ODZs) of the ocean such as found in the eastern tropical Pacific and the Arabian Sea, O_2 concentrations reach nanomolar levels (Revsbech et al. 2009; Thamdrup, Dalsgaard, and Revsbech 2012). These functionally anoxic conditions favor anaerobic microbial pathways (e.g., Dalsgaard et al. 2014) that

1. School for Marine Science and Technology, University of Massachusetts Dartmouth, 706 Rodney French Blvd., New Bedford, MA 02744-1221 USA; orcid: 0000-0003-3120-0710.
2. Corresponding author: ***e-mail: maltabet@umassd.edu***
3. School of the Earth, Ocean, and Environment, University of South Carolina, 701 Sumter Street, Colombia, SC 29208 USA; orcid: 000-0001-7247-5230.

uniquely impact a wide-array of biogeochemical processes including those affecting trace greenhouse gases (e.g., N_2O), trace metals, and, in particular, the microbial production of N_2 by denitrification and anammox. ODZs, despite constituting a small fraction of total oceanic volume (1‰ at $O_2 \leq 20$ μM), play important roles in regulating the global ocean carbon and nitrogen cycles, hosting 30% to 50% of the global loss of biologically available nitrogen to inert N_2 (N-loss; Codispoti and Christensen 1985; Gruber and Sarmiento 1997; Altabet 2007). Any future expansion of ODZs in response to global warming (Stramma et al. 2008, 2009, 2010), often termed "ocean deoxygenation" (Keeling and Garcia 2002), would likely result in feedbacks on fixed nitrogen loss (Horak et al. 2016) and hence ocean productivity.

Up to 15 years ago, heterotrophic denitrification ($NO_3^- \Rightarrow NO_2^- \Rightarrow NO \Rightarrow N_2O \Rightarrow N_2$) by microbes had been considered the primary microbial pathway for N-loss and production of biogenic N_2 gas. More recently, chemosynthetic anammox ($NO_2^- + NH_4^+ \Rightarrow N_2 + 2H_2O$) has also been recognized as a source of biogenic N_2 in ODZs but requiring NH_4^+ and NO_2^- to be produced by other processes. Although NH_4^+ concentrations are almost always very low in ODZs (> tenths of μmol kg^{-1}), the buildup of NO_2^- is thought required for biogenic N_2 production regardless of pathway (Lam et al. 2009; Bristow et al. 2017), and the secondary NO_2^- maxima (1 to 10 μmol kg^{-1}) has always been seen as a key indicator of active N-loss in ODZs (e.g., Codispoti and Packard 1980).

A number of ^{15}N tracer-rate experiments and studies using molecular techniques to characterize the ODZ microbial community have indicated that instead of denitrification, anammox is the major pathway for N-loss in ODZs (Dalsgaard, Thamdrup, and Canfield 2005 and references therein). Nevertheless, there are other modern tracer studies that continue to support heterotrophic denitrification as the major source of biogenic N_2 in ODZs (Ward et al. 2009; Babbin et al. 2014). In addition, there is evidence that denitrification may occur primarily as large sporadic events over a low-level background of anammox (Dalsgaard et al. 2012). Consequently, part of the inconsistencies between studies may result from temporal/spatial aliasing.

Richards (1965) first considered theoretically an overall stoichiometry for ODZ N-loss. His approach was an extension of Redfield's (1934) discovery of the oceans having an average stoichiometry between C, O, N, and P in the cycle of organic matter production and regeneration. This innovation resulted in the invention of "biogeochemistry" and led to realization of the coregulating nature of these elemental cycles. The corresponding specific stoichiometric parameters are now essential to modern models of biogeochemical cycles including those of the ocean's biological carbon pump. Similar logic applies to N-loss in ODZs and based on the assumption of Redfield elemental composition for respired organic matter, Richards quantitatively related the consumption of organic matter and NO_3^- to production of CO_2, N_2, and PO_4^{-3}:

$$(CH_2O)_{106}(NH_3)_{16}H_3PO_4 + 94.4\ HNO_3 = 106\ CO_2 + 55.2\ N_2 + 177.2\ H_2O + H_3PO_4. \quad (1)$$

Equation (1) predicts a biogenic N_2 production (in N units) to NO_3^- consumption ratio of 1.17 and a biogenic N_2 (in N units) to PO_4^{-3} production ratio of 110.4. Because NH_4^+ was known to not significantly accumulate in ODZs, Richards inferred its transformation to N_2, and thus the anammox pathway was implied decades before its discovery. Alternative equations to equation (1) with modest modifications have been suggested (Codispoti and Packard 1980); nevertheless, from equation (1) it follows that there is a predicted ratio of NO_3^- consumed to N_2 produced depending on the elemental composition of organic matter (Chang, Devol, and Emerson 2010). Equation (1) also implies that the relative importance of anammox and denitrification is similarly determined by the proportional contribution of NH_4^+ to N_2 production, in this case ∼15% (Babbin et al. 2014). High rates of anammox relative to denitrification in ODZs (anammox has been reported to account for all N_2 production in the Peru ODZ; Hamersley, Lavik, and Woebken 2007) would require additional sources of NH_4^+ to be identified. The ratio of NO_3^- ($+NO_2^-$) consumed to N_2 produced thus places a robust observable constraint on the relative biogeochemical importance of these processes. The few published studies so far support the N stoichiometry in equation (1) (Chang, Devol, and Emerson 2010, 2012; Bourbonnais et al. 2015) suggesting a fundamental gap in our understanding of ODZ N-loss biogeochemistry with respect to dominant microbial pathways.

To examine N-loss stoichiometry in situ, we exploit here observations made of a mesoscale eddy within the Peru ODZ that had experienced an extreme degree of N-loss (Bourbonnais et al. 2015). Mesoscale eddies generally can have extensive impacts on biological and biogeochemical processes. In oligotrophic gyres, they enhance primary productivity by "eddy pumping," the local upwelling of nutrients to the euphotic zone (Falkowski et al. 1991; McGillicuddy et al. 1998, 2007; Oschlies and Garçon 1998). Given dependence on organic matter flux (Ward et al. 2008; Kalvelage et al. 2013; Babbin et al. 2014), impact on ODZ N-loss is, in hindsight, sensible. Altabet et al. (2012) observed extreme N-deficit, buildup of biogenic N_2, NO_2^- concentrations, and high NO_3^- isotope enrichment at a station at the edge of an anticyclonic eddy that was the first evidence for eddy N-loss hot-spot activity in ODZs. These observations are likely general as there have been reports of other eddy systems that, once detached from coastal current systems, either retain or achieve ODZ conditions and accumulate N-loss biogeochemical signatures (e.g., Cornejo D'Ottone et al. 2016; Callbeck et al. 2017).

We have been able to follow up on this finding with more highly resolved observations of intense N-loss and associated isotopic signals in a near-coastal eddy off Peru sampled in November and December 2012 (referred to as "Eddy A" in Stramma et al. 2013; Bourbonnais et al. 2015). We observed extreme N-loss signals in the center of Eddy A, and we use the covariation in NO_3^- ($+NO_2^-$), biogenic N_2, and PO_4^{-3} to examine the relevance of Richards's stoichiometry to this system. An inherent advantage of this approach that complements tracer and microbial studies is that the observed biogeochemical signals represent the integration of microbial processes over relatively long timescales (as compared with tracer incubations). In this case, integration time is approximately the lifetime of the

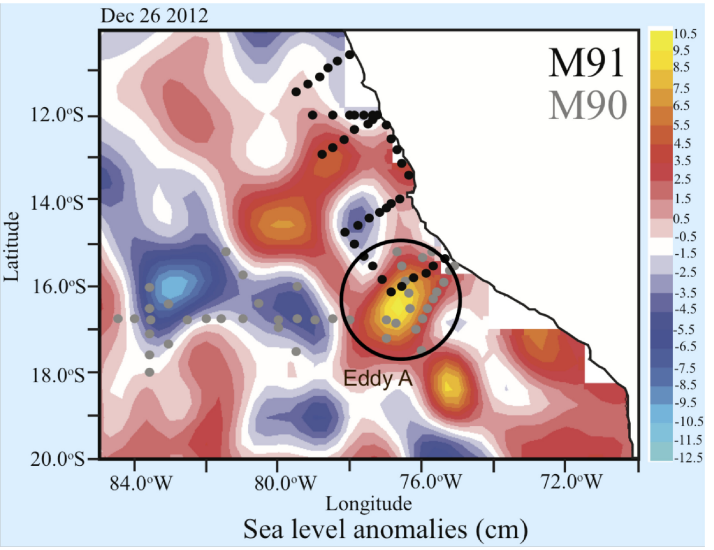

Figure 1. Map showing stations sampled during the M90 (gray dots) and M91 (black dots) cruises. Contours indicate the delayed time, 7-day, mean sea level anomalies (SLAs; in cm) centered on 26 December 2012. The transects of Eddy A used for our analysis are shown within the circle. SLA data are from Aviso (http://www.aviso.oceanobs.com).

eddy—2 to 3 months. Bourbonnais et al. (2015) was the first to examine the natural isotope (^{15}N) mass balance between NO_3^- ($+NO_2^-$) and biogenic N to consider the isotope fractionation effects during N-loss. Here, we extend this approach to further test assumptions regarding N sources and sinks in consideration of N-loss stoichiometry. Using an eddy N-loss hot spot in this way has the distinct advantages of intense biogeochemical signatures, relatively well-defined timescales, and simplified hydrography.

2. Sample collection and methods

a. Sampling regime and hydrographic data

Mesoscale eddies within the Peru ODZ were studied during two research cruises aboard the R/V *Meteor* late November (M90) and late December (M91) 2012 (Fig. 1), as part of the German projects SFB 754 ("Climate-Biogeochemistry Interactions in the Tropical Ocean": http://www.sfb754.de) and SOPRAN ("Surface Ocean Processes in the Anthropocene": http://www.sopran.pangaea.de). The presence and locations of the several eddies surveyed were confirmed by satellite data for sea level anomaly (SLA), sea surface temperature, and chlorophyll a (Stramma et al. 2013). As in the Bourbonnais et al. (2015) study of N isotope effects, we only consider the most coastal anticyclonic, mode-water eddy observed during both cruises (corresponding to Eddy A in Stramma et al. 2013; Fig. 1), because of its intense N-loss signals (Stramma et al. 2013).

Water samples were collected at every station close to or within the eddy (transects shown in Fig. 1) using 12 L Niskin bottles (~23 depths/profile) on a CTD rosette equipped with pressure, conductivity, temperature, and O_2 sensors. Oxygen and nutrients (NO_3^-, NO_2^-, NH_4^+, and PO_4^{3-}) were measured onboard as described in Stramma et al. (2013). Nitrogen deficits relative to PO_4^{-3} (N'p) were calculated as in Bourbonnais et al. (2015):

$$\text{N'p} = 15.8 \times ([PO_4^{3-}] - 0.3) - NO_3^- - NO_2^-, \quad (2)$$

which takes into account preformed N'p in the eastern tropical South Pacific Ocean. NH_4^+ was always either nondetectable or at concentrations <0.5 μmol kg^{-1} and hence was not included in the calculation. Nitrous oxide (N_2O), an intermediate during denitrification, only accumulated up to ~90 nmol L^{-1} (0.09 μmol L^{-1}) in the coastal eddy (Arévalo-Martínez et al. 2016) and is thus also not considered in our isotopic mass balance.

Samples for NO_3^- isotopic composition were collected in 125 mL plastic bottles and acidified for preservation (1 mL of 2.5 mM sulfamic acid in 25% HCl). Any NO_2^- present in these samples was removed by the sulfamic acid (Granger and Sigman 2009). For NO_2^- isotopic analysis, a separate set of samples was collected and preserved with NaOH and frozen until analysis (Casciotti et al. 2007). Samples for N_2/Ar and δ^{15}N-N_2 were collected in 60 mL serum glass bottles, sealed without headspace with butyl rubber stoppers, and preserved with 100 μL $HgCl_2$ (Charoenpong, Bristow, and Altabet 2014). Duplicate or triplicate samples were collected either at all stations (M90) or every other station (M91).

b. Isotopic composition of NO_3^- and NO_2^-

The stable isotopic compositions of NO_3^- and NO_2^- were analyzed using the "azide method" as described in McIlvin and Altabet (2005), with 10% of the total number of samples analyzed as duplicates. Although both δ^{15}N and δ^{18}O were measured, here we focus on δ^{15}N in consideration of ^{15}N mass balances. For NO_3^- isotopic analysis, cadmium was first used for the reduction of NO_3^- to NO_2^-. For both NO_3^- and NO_2^- isotopic analysis, NO_2^- was converted to nitrous oxide (N_2O) using sodium azide in acetic acid. N_2O gas was automatically extracted, purified, and analyzed on-line using a purge-trap preparation system coupled to an IsoPrime continuous-flow, isotope ratio mass spectrometer (CF-IRMS). The target sample and standard size was 15 nmol N_2O. N isotope ratios are reported using the "δ" notation in per mil (‰) units, relative to N_2. Standardization and quality control were as in Bourbonnais et al. (2015).

Reproducibility was generally better than 0.2‰ for δ^{15}N.

c. N_2/Ar and δ^{15}N-N_2 measurements

High-precision measurements of N_2/Ar and the δ^{15}N of N_2 ($\delta^{15}N_2$) were made using an on-line gas extraction system coupled to a multicollector CF-IRMS as described in Charoenpong, Bristow, and Altabet (2014). O_2 was removed from the samples prior to $\delta^{15}N_2$ analysis using a CuO/Cu reduction column placed in a 500°C furnace to avoid

interferences caused by interaction between O_2, N_2, and their fragments within the IRMS ion source. Excess N_2 concentration ($[N_2]_{excess}$) in μmol L^{-1}, the observed $[N_2]$ minus the equilibrium $[N_2]$ at *in situ* temperature and salinity, was calculated as in Charoenpong, Bristow, and Altabet (2014) and calibrated daily against seawater standards equilibrated with air at fixed temperature. Precision of the measurements (standard deviation) for the samples was generally better than 0.7 μmol L^{-1} for $[N_2]_{excess}$ and 0.03‰ for $\delta^{15}N\text{-}N_2$.

d. Derived parameter calculations

We calculated biogenic $[N_2]$ ($[N_2]_{biogenic}$), the $[N_2]$ produced by denitrification or anammox, by subtracting the $[N_2]_{excess}$ measured at a background station unaffected by N-loss ($[O_2]$ >10 μmol L^{-1}) located north of the ODZ (1.6° N, 85.83° W; M90 cruise) from the observed $[N_2]_{excess}$ at corresponding σ_θ (Bourbonnais et al. 2015). This corrects for nonlocal biological N-loss and physically produced deviations in equilibrium N_2/Ar (e.g., bubble injection at remote water mass outcrop regions; see Hamme and Emerson 2002).

The $\delta^{15}N$ of biogenic N_2 ($\delta^{15}N_{2\ biogenic}$, in ‰) was calculated by mass balance:

$$\delta^{15}N_{2measured} \times [N_2]_{measured} = \delta^{15}N_{2equil} \times [N_2]_{equil} + \delta^{15}N_{2biogenic} \times [N_2]_{biogenic}, \quad (3)$$

$$\delta^{15}N_{2biogenic} = (\delta^{15}N_{2measured} \times [N_2]_{measured} - \delta^{15}N_{2equil} \times [N_2]_{equil})/[N_2]_{biogenic}, \quad (4)$$

where $\delta^{15}N_{2equil}$ and $[N_2]_{equil}$ are the equilibrium $\delta^{15}N_2$ and $[N_2]$ at *in situ* temperature and salinity, respectively. $[N_2]_{measured}$ is $[N_2]_{equil}$ + $[N_2]_{excess}$, and $\delta^{15}N_{2measured}$ is the directly measured value.

3. Results and discussion

a. Eddy A characteristics

As described previously (Stramma et al. 2013), Eddy A was a mode-water eddy, a hybrid between anticyclonic and cyclonic eddies, in proximity to the Peru Margin. Being colocated with maxima in SLA, overall rotation was anticyclonic (Fig. 1). Its deeper isopycnal surfaces between 150 and 500 m were depressed downward at the eddy's center by up to 100 m giving the eddy its overall anticyclonic rotation as dictated by geostrophy (Fig. 2a). However, between 50 and 150 m, isopycnal surfaces bowed upward resulting in a 50 m shoaling of the oxycline. Mode-water eddies of the Peru Margin appear to be formed by instabilities of the Peru Undercurrent (PUC) as it bends around critical angles imposed by the shape of the coastline particularly in the vicinity of 15° S (Chaigneau, Gizolme, and Grados 2008). Eddies formed in this way have an upper portion derived from the Peru Coastal Current (PCC) and a lower portion from the PUC, which give them their mode-water characteristics. Time-series SLA data indicate that Eddy A was 2 months (M90) and 3 months (M91) old when observed.

Hydrographically, Eddy A is very similar to its water mass sources from the PCC and PUC being mostly composed at its core of water from Antarctic Intermediate Water at

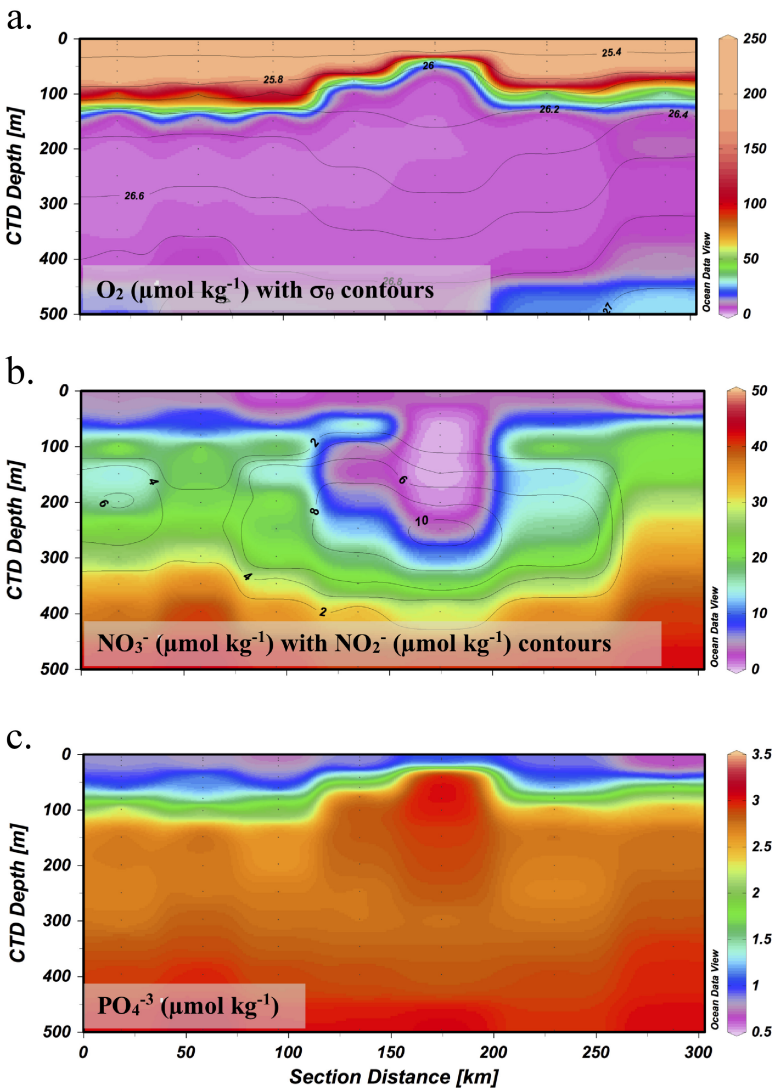

Figure 2. Section plots through Eddy A during M90 showing [O_2] (µmol kg^{-1}) with σ_θ (kg L^{-1}) overlaid as contours (a), NO_3^- (µmol kg^{-1}) overlaid with NO_2^- (µmol kg^{-1}) contours (b), and PO_4^{-3} (µmol kg^{-1}) (c).

depth, Equatorial Subsurface Water in its core, and Subtropical Surface Waters near surface as shown by simple *T*-*S* mixing lines for data from both M90 and M91 (Fig. 3a). *T*-*S* points that fall off the mixing line are from the eddy's periphery toward the coast and probably reflect shelf modification of temperature and/or salinity. Noteworthy is that all of the *T*-*S*

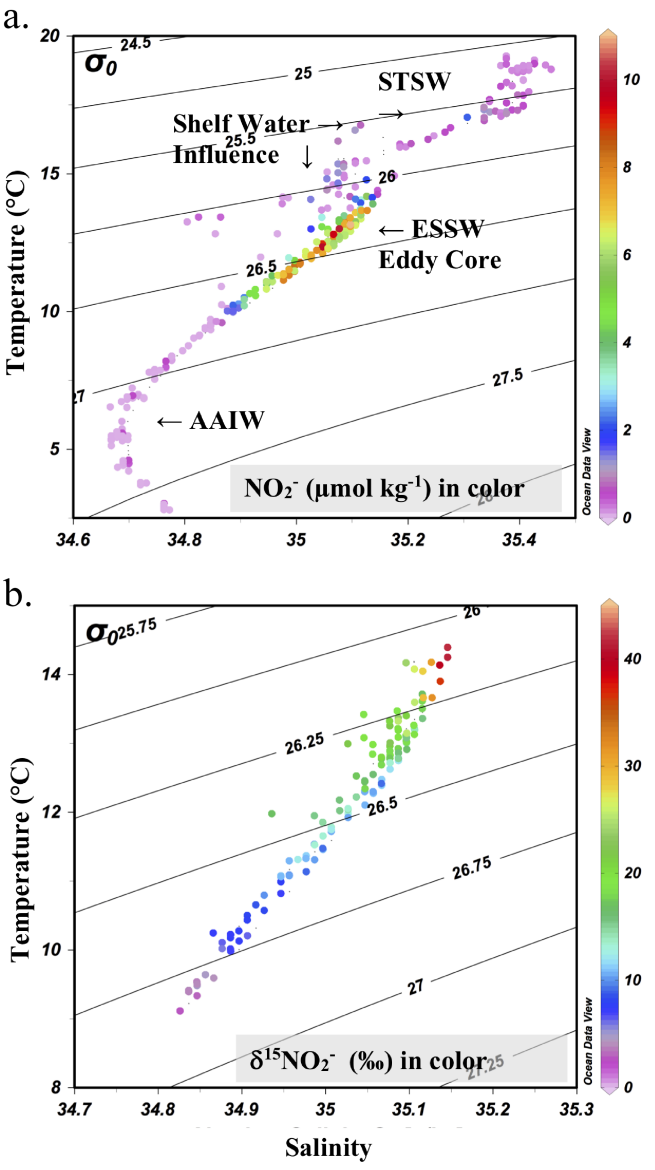

Figure 3. Temperature (°C) versus salinity diagram for Eddy A and surroundings. (a) Water mass sources from Antarctic Intermediate Water (AAIW), Equatorial Subsurface Water (ESSW), and Subtropical Surface Water (STSW) are shown. Points indicating shelf water influence are also annotated. Color indicates $[NO_2^-]$ (μmol kg^{-1}). (b) Subset of points with detectable NO_2^- with color indicating $\delta^{15}NO_2^-$ (‰).

points with elevated NO_2^- from the eddy core region fall on a simple mixing line. NO_2^- is an intermediate in the reduction of NO_3^- to N_2, and its presence is required for active denitrification (Bristow et al. 2017).

In this region of the Peru ODZ, O_2 is uniformly depleted between ~100 and 450 m, but within Eddy A, the O_2-deficient zone is distinctly thicker (Fig. 2a). Micromolar O_2 is also found on less dense isopycnal surfaces in the eddy center indicating a local intensification of ODZ conditions and that the shoaling of oxycline is not purely a physical phenomenon. Indeed, the eddy center clearly experienced an intensification of N-loss. The eddy center is nearly NO_3^- depleted as compared with values ~20 μmol kg^{-1} in surrounding waters at comparable depth and isopycnal surface (Fig. 2b). Where NO_3^- is most depleted, biogenic N_2 is maximal (see Bourbonnais et al. 2015). NO_2^- also reaches higher levels within the eddy with values as high as 10 μmol kg^{-1}, though centered below the region of extreme NO_3^- depletion (Fig. 2b). Further evidence of denitrification intensification in the upper eddy core is the PO_4^{-3} maximum of >3 μmol kg^{-1} colocated there (Fig. 2c). This is one of the strong biogeochemical signals present in the eddy N-loss "hot spot" that we will use in consideration of the stoichiometry found in equation (1).

As nitrate reduction is accompanied by relatively strong isotope effects (20‰ to 30‰; Brandes et al. 1998; Voss, Dippner, and Montoya 2001; Granger et al. 2008), large ^{15}N enrichments accompany NO_3^- depletion (Fig. 4). As with the other biogeochemical indicators of N-loss, the most extreme $\delta^{15}N$ values are colocated in the upper core of Eddy A for NO_3^-, NO_2^-, and N_2. As the primary source for N-loss, NO_3^- is expected to become ^{15}N enriched with depletion with the intermediate NO_2^- being offset to lower values. Figure 2(b) shows the highest $\delta^{15}N$ NO_2^- values on the least dense (shallowest) density surfaces within the eddy's core waters. As the ultimate product, N_2 is initially ^{15}N depleted at lower levels of NO_3^- removal as seen in the lower region of the eddy core, as well as in surrounding waters. As NO_3^- removal becomes almost complete, N_2 in the upper eddy core also becomes ^{15}N enriched. The overall $\delta^{15}N$ range for N_2 is highly truncated as compared with NO_3^- and NO_2^- because of dilution by the background N_2 of atmospheric origin. Bourbonnais et al. (2015) used this ^{15}N data to verify assumptions underlying estimates of isotope fraction. Here, we use them to test assumptions underlying our evaluation of N-loss stoichiometry.

There are a number of possible mechanisms that could be responsible for Eddy A becoming an N-loss hot spot. Previously, it was noted that satellite images show high chlorophyll-a surface shelf waters being pulled offshore and wrapping around eddy peripheries (Altabet et al. 2012). Such offshore surface transport of near-surface productivity would likely translate into high organic matter flux inside the eddy, stimulating N-loss (Stramma et al. 2013). Alternatively, the shoaling oxycline at the eddy center could stimulate local productivity by bringing nutrient-rich water into the euphotic zone as suggested by the loss of O_2 on lower density surfaces within the eddy. To the degree productivity is limited by nitrogen as opposed to phosphorous or micronutrients such as iron, this mechanism would be self-limiting with high degrees of N-loss as observed in Eddy A. This would account for little further N-loss

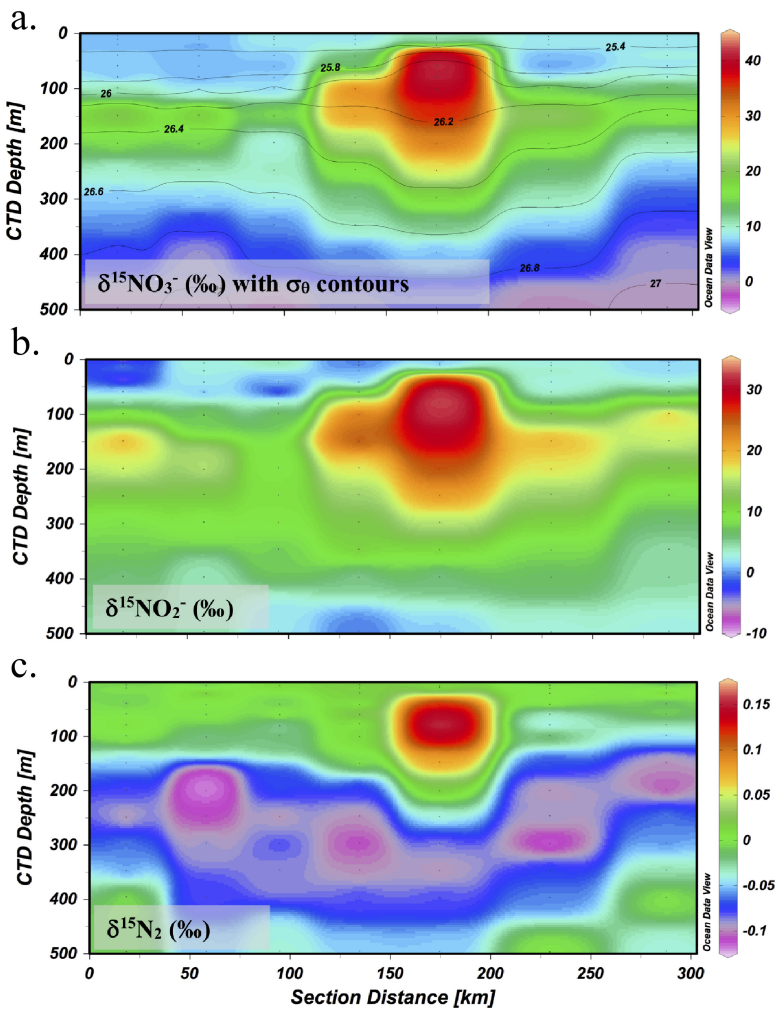

Figure 4. Section plots through Eddy A during M90 showing $\delta^{15}NO_3^-$ (‰) with σ_θ (kg L^{-1}) overlaid as contours (a), $\delta^{15}NO_2^-$ (‰) (b), and $\delta^{15}N_2$ (‰) (c).

between the M90 and M91 observations. Even without enhanced organic matter availability, increased N-loss would be expected as a result of a shoaler oxycline as O_2-deficient waters would be exposed to greater particle flux from simply being higher up on the "Martin curve" (Martin et al. 1987; Yang et al. 2017). Unfortunately, these hypotheses remain untested as no study of eddy N-loss hot spots targeting potential mechanisms has yet been carried out.

As nearby, shallow Peru shelf waters can experience extreme N-loss (Hu et al. 2016), eddy N-loss hot-spot conditions could be explained more mundanely by shelf water

capture during eddy formation. However, several lines of evidence refute this: (1) As cited previously, eddy core T-S characteristics are consistent with a PUC source (Fig. 3). (2) Shallow shelf waters generate high silicate anomalies because of fluxes from the sediments. No such anomalies were observed in Eddy A. (3) Shelf waters have been shown to have a suppressed NO_3^- isotopic fractionation effect likely because of contributions from sediment N-cycling (Hu et al. 2016), whereas the magnitude of this effect in Eddy A was similar to the rest of the offshore Peru ODZ (Ryabenko et al. 2012; Casciotti, Buchwald, and McIlvin 2013; Bourbonnais et al. 2015). Accordingly, the extreme N-loss signals observed in Eddy A were most likely generated after formation by in situ processes.

b. N-loss stoichiometry

i. ^{15}N mass balance. Before comparing theoretical and observed N-loss stoichiometries, we first test the assumption that biogenic N_2 is derived primarily from the reduction of NO_3^- (with NO_2^- as an intermediary) with more minor contributions from organic N as indicated by equation (1). To do so, we take advantage of the N isotope fractionation observed to occur during N-loss, which we have shown produces large variations in $\delta^{15}N$ because of (a) the large fractionation potential associated with NO_3^- reduction and (b) the large degree of NO_3^- removal. Hence, in the absence of large contributions from organic N (via NH_4^+ and anammox) as in equation (1), the $\delta^{15}N$ of biogenic N_2 should be predicted by the concentration weighted change in the $\delta^{15}N$ of $NO_3^- + NO_2^-$:

$$\delta^{15}N_{2bio} \times 2 \times [N_{2bio}] \sim (\delta^{15}NO_3^- \times [NO_3^-] + \delta^{15}NO_2^- \times [NO_2^-])_{initial} - (\delta^{15}NO_3^- \times [NO_3^-] + \delta^{15}NO_2^- \times [NO_2^-])_{observed}. \quad (5)$$

Initial $\delta^{15}N$ and concentration values are taken from observations outside the ODZ at the same isopycnal surfaces as the observation.

A plot of measured $\delta^{15}N_{2\,bio}$ versus values expected from equation (3) shows a strong correlation ($r^2 = 0.75$) with slope derived by linear regression slightly less than 1 (0.88; Fig. 5a). The intercept of -0.75 is relatively small and not statistically significant. The greater scatter about the linear regression line for the lower $\delta^{15}N_2$ values is primarily methodological as here biogenic N_2 values are small relative to background leading to greater analytical uncertainty. Restricting analysis to points with biogenic $[N_2] > 15$ μmol kg^{-1} results in a tighter correlation ($r^2 = 0.88$) with slope indistinguishable from 1 (Fig. 5b). Effectively, this restriction focuses on the eddy core with N-loss hot-spot conditions.

These results support a simple scenario of increasing conversion of NO_3^- (+ NO_2^-) to N_2 from the eddy periphery to its core with an approximate quantitative balance between the two. However, our analysis probably does not have sufficient sensitivity to detect the modest contributions from organic N indicated in equation (1). These results do indicate that anammox as currently understood cannot be the dominant process for N_2 production as

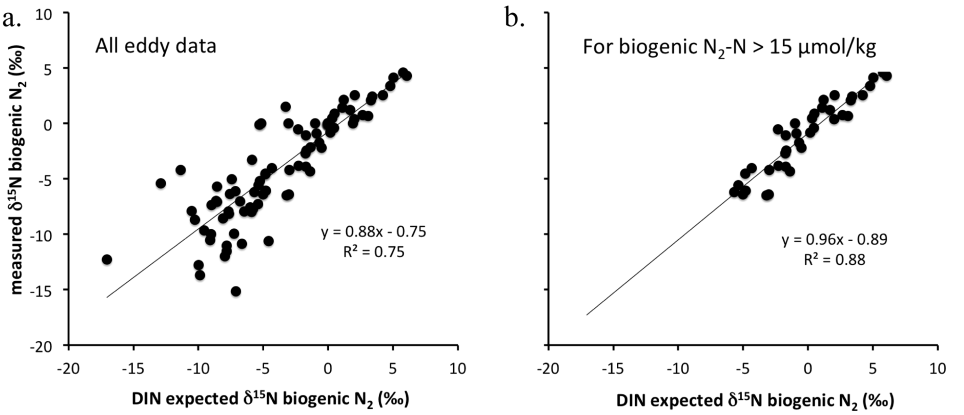

Figure 5. Cross plots of Eddy A data of the measured δ^{15}N (‰) of biogenic N_2 versus expected values from the δ^{15}N measurements of NO_3^- and NO_2^- (see text for explanation): all data for Eddy A (a) and data for [biogenic N_2-N] >15 µmol kg^{-1} (b).

suggested by a number of studies including tracer-rate measurements in Eddy A (Callbeck et al. 2017) as about half the nitrogen in biogenic N_2 would need to come from NH_4^+ derived from organic matter. In contrast, if NH_4^+ derived from organic matter was a major contributor to biogenic N_2, the slope in Figure 5 would be significantly different from 1. This would be the case regardless of its specific δ^{15}N values as a whole term would be missing from the right-hand side of equation (4). We carried out hypothetical calculations over a range in anammox contributions to N_2 production from 15% (Richards's stoichiometry) to 50%, assuming the organic nitrogen source for biogenic N_2 had δ^{15}N values of 7‰. We found that Figure 5 slopes would range from 0.86 to 0.43, respectively, and the reduction in slope would be even more extreme if the δ^{15}N for organic N was even greater.

ii. Nitrogen balance. Having examined the ^{15}N mass balance for N-loss in Eddy A, we now consider the nitrogen balance between the removal of NO_3^- (+ NO_2^-) and production of biogenic N_2. Two approaches are used to assess NO_3^- removal, the first being the conventional N deficit (N'p) approach as given in equation (2), which estimates the "missing" NO_3^- (+ NO_2^-) relative to the amount expected from observed PO_4^{-3} concentrations assuming near-Redfield stoichiometry. The second approach examines the change in $NO_3^- + NO_2^-$ and assumes a constant initial $[NO_3^- + NO_2^-]$ concentration relying on the well-constrained hydrography of the eddy and the large gradients developed along isopycnal surfaces over small horizontal distances. This second approach is insensitive to non-N-loss influences on P-cycling such as variation in organic matter N:P ratio.

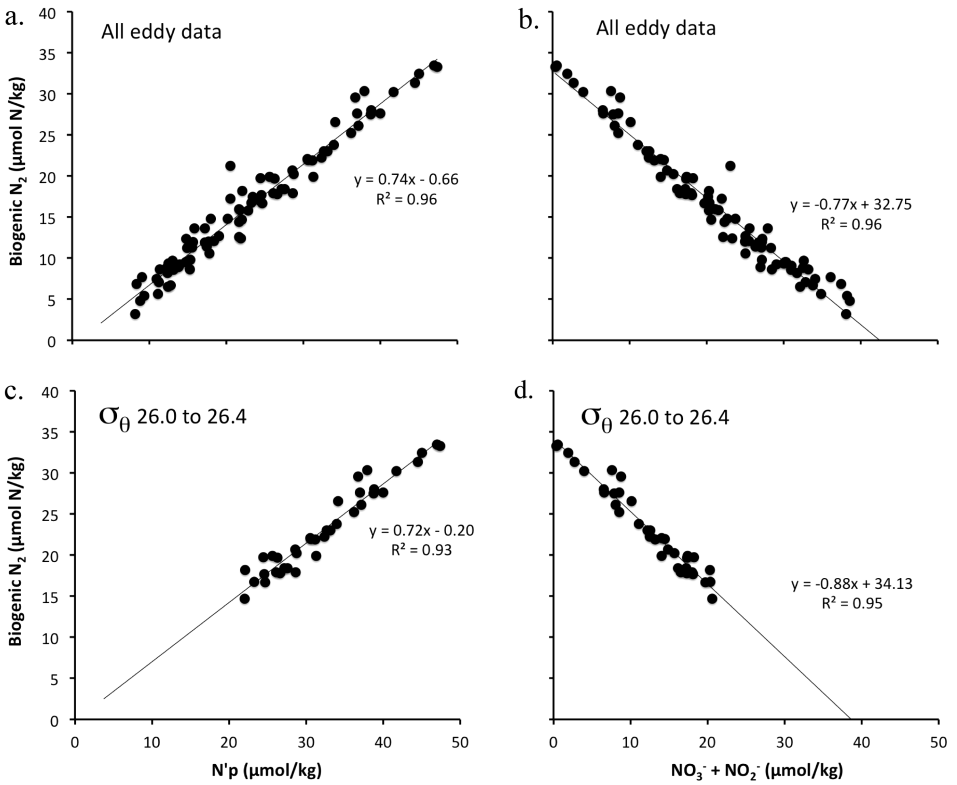

Figure 6. Cross plots of Eddy A data of the measured [biogenic N_2-N] (μmol kg^{-1}) versus two measures of N-loss. (a) Against N'p (μmol kg^{-1}) for all eddy data. (b) Against [NO_3^- + NO_2^-] (μmol kg^{-1}) for all eddy data. (c) Against N'p (μmol kg^{-1}) for σ_θ (kg L^{-1}) 26.0 to 26.4. (d) Against [NO_3^- + NO_2^-] (μmol kg^{-1}) for σ_θ (kg L^{-1}) 26.0 to 26.4.

In Figure 6(a), biogenic N_2 (in N units) is highly linearly correlated with N'p for all eddy data with an r^2 of 0.96. A relatively small intercept of -0.66 indicates no large systematic offsets. Equations (1) and (2) predict a slope of $\sim$1 as any biogenic N_2 derived from organic N is taken into account by the PO_4^{-3} produced via equation (2). Hence, the slope of 0.74 is surprising as it indicates that $\sim$25% less N_2 is produced than predicted in contrast to our expectation that anammox dominance would produce slopes greater than 1. In Figure 6(c), we restrict the data to the σ_θ range 26.0 and 26.4 to both focus on the eddy upper core region and test whether there is any influence from water mass mixing. This restriction produces no significant difference in results.

In Figure 6(b), biogenic N_2 (in N units) is also highly linearly correlated with NO_3^- + NO_2^- with an r^2 of 0.96 but also with a slope of -0.77. Here too, less biogenic N_2 appears to have been produced as compared with expectations from equation (1), which predicts

that 16% of the biogenic N_2 originates from organic N (expected slope = -1.17). If somehow biogenic N_2 only came from the reduction of NO_3^- and NO_2^-, then the expected slope would be -1.0. As before, restriction of the data set considered to the σ_θ range 26.0 and 26.4 (Fig. 6d) shows little change in the relationship between increasing biogenic N_2 and decreasing $NO_3^- + NO_2^-$, though the slope is now slightly closer to -1.0 (-0.88). Overall these results show that less biogenic N_2 is produced than expected from equation (1) regardless of whether the comparison is with the N deficit (N'p) or the disappearance of $NO_3^- + NO_2^-$.

iii. PO_4^{-3} *stoichiometry.* Our results strongly suggest that Richards's stoichiometry does not strictly hold for eddy N-loss hot spots and perhaps more generally for the Peru ODZ. A further clue in this regard is found in the accumulation of PO_4^{-3} in the eddy core, which must result from N-loss as a net heterotrophic process. As before, we examine the stoichiometry of PO_4^{-3} production with cross plots of biogenic N_2 versus PO_4^{-3} and $NO_3^- + NO_2^-$ versus PO_4^{-3} with isopycnal restriction.

In Figure 7(a), a more complicated relationship is observed between biogenic N_2 and PO_4^{-3} than in our prior analyses. However, data restriction to the σ_θ range 26.0 and 26.4 shows the qualitatively expected relationship of PO_4^{-3} increasing with biogenic N_2. We surmise that the all-eddy-data plot in Figure 7(a) includes deeper density surfaces with decreasing biogenic N_2 but increasing pre-N-loss PO_4^{-3} that produces the trend in the lower third of the plot. In Figure 7(b), the slope of 51 is much less than the expected value of 110 from equation (1) indicating higher than expected PO_4^{-3} production during N-loss.

In Figure 7(c) and (d), similar observations are made in the relationship between $NO_3^- + NO_3^-$ and PO_4^{-3}. In this instance, the positive correlation between NO_3^- and PO_4^{-3} typical for non-N-loss waters is seen in the upper third of Figure 7(c) and is apparent from inspection of the >300 m region of Figure 2 where increases with depth are dominant. The restriction to σ_θ range 26.0 and 26.4 in Figure 7(d), by contrast, emphasizes the correlated decrease in $NO_3^- + NO_2^-$ with increasing PO_4^{-3} occurring horizontally from outside to inside the upper eddy core.

4. Synthesis and conclusions

We have observed extreme N-loss in a mode-water eddy within the Peru ODZ. We speculate that a combination of enhanced organic matter flux and relative isolation from surrounding waters facilitated the occurrence of almost complete conversion of NO_3^- to biogenic N_2 within the eddy's upper core. Here we take advantage of these characteristics to use Eddy A as a natural laboratory to study N-loss stoichiometry. This approach regarding the study of eddies was first applied to warm core rings (WCRs) of the Gulf Stream region in an interdisciplinary research program promulgated by James J. McCarthy (e.g., Altabet and

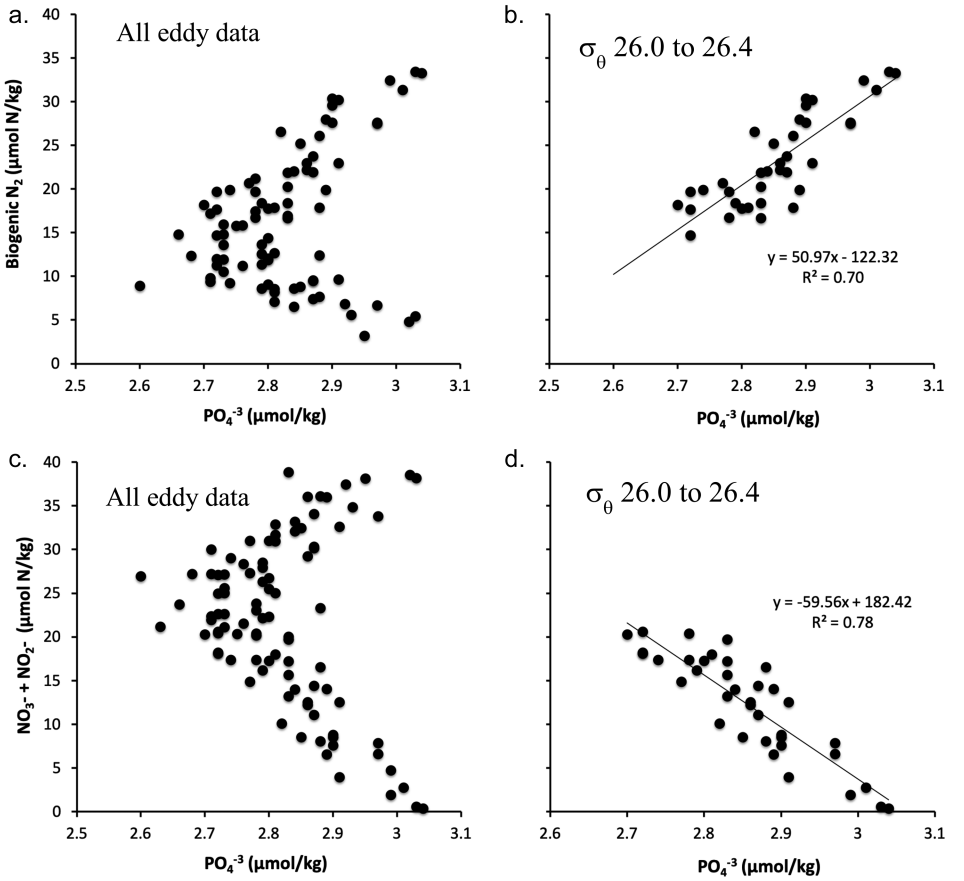

Figure 7. Cross plots of Eddy A data of two measures of N-loss against PO_4^{-3}. (a) Biogenic N_2 (μmol kg^{-1}) versus PO_4^{-3} (μmol kg^{-1}) for all eddy data. (b) Biogenic N_2 (μmol kg^{-1}) versus PO_4^{-3} (μmol kg^{-1}) for σ_θ (kg L^{-1}) 26.0 to 26.4. (c) NO_3^- + NO_2^- (μmol kg^{-1}) versus PO_4^{-3} (μmol kg^{-1}) for all eddy data. (d) NO_3^- + NO_2^- (μmol kg^{-1}) versus PO_4^{-3} (μmol kg^{-1}) for σ_θ (kg L^{-1}) 26.0 to 26.4.

McCarthy 1985) who was the first author's PhD advisor for his thesis on WCR N-isotope dynamics.

The approximately twofold excess PO_4^{-3} generated in Eddy A would appear to support anammox as a dominant process producing biogenic N_2. Greater PO_4^{-3} regeneration from organic matter implies greater availability of NH_4^+ for anammox than expected from Richards's stoichiometry. An extreme scenario that could account for the tracer-rate results would be one in which all the NO_2^- produced by NO_3^- reduction combines with NH_4^+

(produced by an unknown heterotrophic process). For NO_3^- reduction to NO_2^- only,

$$212\ HNO_3 + (CH_2O)_{106}(NH_3)_{16}H_3PO_4 = 106\ CO_2 + 212\ HNO_2 + 106\ H_2O + 16\ NH_3 + H_3PO_4. \quad (6)$$

Given that the breakdown of organic matter needed to produce the necessary NH_4^+ would also produce PO_4^{-3}, the expected overall N_2-N:PO_4^{-3} under this scenario would be 16:1, much less than our observations of ~50:1 The same N_2-N:PO_4^{-3} production ratio would result if the "excess" NO_2^- over NH_4^+ produced in equation (5) was instead oxidized back to NO_3^-, a possibility given the persistent observation of this process within ODZs (Casciotti, Buchwald, and McIlvin 2013; Bourbonnais et al. 2015). Given the observed N_2-N:PO_4^{-3}, a reasonable conclusion would be that about 50% of N_2 production is from denitrification and 50% is from anammox based on these data alone.

However, the ^{15}N and N concentration balance data between NO_3^- + NO_2^- and biogenic N_2 indicate otherwise. Both suggest little contribution to biogenic N_2 from sources other than the reduction of NO_3^- and NO_2^-. In fact, the N budget analysis suggests that about 20% of the NO_3^- + NO_2^- removal is "missing" with respect to biogenic N_2 production. One way to make sense of these apparent contradictory results is to reconsider the assumption of Redfield stoichiometry for the organic matter oxidized by NO_3^- in equation (1). If the organic N:P was 9 to 10 instead of 16, in equation (1), the observed N_2-N:PO_4^{-3} would be predicted without any "extra" anammox. P-rich organic matter is likely produced in the Peru upwelling system as water upwelling from the ODZ is obviously N-poor.

Another possibility that has been considered is that the "extra" NH_4^+ needed by anammox is supplied by dissimilatory nitrate reduction to ammonia (DNRA; $NO_3^- \Rightarrow NO_2^- \Rightarrow NH_4^+$), a heterotrophic microbial process known in the terrestrial environment but generally not considered important in open marine systems. Lam et al. (2009) and Lam and Kuypers (2011) using ^{15}N tracer experiments measured significant rates of DNRA in the Peru ODZ and proposed this pathway as an important source of NH_4^+ for anammox. However, subsequent studies did not confirm this finding (Kalvelage et al. 2013). The stoichiometry for DNRA assuming organic matter with Redfield composition is

$$53\ HNO_3 + (CH_2O)_{106}(NH_3)_{16}H_3PO_4 = 106\ CO_2 + 53\ H_2O + 69\ NH_3 + H_3PO_4. \quad (7)$$

According to equations (6) and (7), when there is 2.84 times more DNRA than NO_3^- reduction to NO_2^-, equal amounts of NO_2^- and NH_4^+ are produced. This scenario would support all biogenic N_2 production via anammox. The biogenic N_2 production to NO_3^- consumption ratio would be 1.17, and the biogenic N_2 to PO_4^{-3} production ratio would be 110.4. These ratios are the same as from Richards's stoichiometry! Though involving different microbial pathways, the biogeochmical result is indistinguishable whether heterotrophic denitrification is the sole pathway or if instead there was a combination of NO_3^- reduction to NO_2^-, DNRA, and anammox. To explain the observed biogenic

N_2 to PO_4^{-3} ratio, we still need to call on a role for non-Redfield composition organic matter.

We are left with the issue of the "missing" biogenic N_2. Mixing and exchange between the eddy core and its periphery would reduce biogenic N_2 but at the same time increase $NO_3^- + NO_2^-$ making their correlation relatively insensitive to physical exchange. If instead biogenic N_2 was lost to the atmosphere, there would be no corresponding gain of $NO_3^- + NO_2^-$, yielding reduced regression slopes as observed. However substantial air-sea gas exchange seems unlikely to affect the region of maximal biogenic N_2 as this region remained O_2 depleted. Potential artifacts affecting just the biogenic N_2 results are diminished or eliminated by the analysis along an isopycnal surface with little to no variation in T and S (Fig. 6c and d). The physical N_2 excess is calculated as a function of density and hence would not vary among these data. As this value is subtracted from the measured excess N_2 to derive biogenic N_2, an error in this value would influence the intercept but not the slope in Figure 6(c) and (d). Mixing between waters varying in T and S and hence equilibrium $[N_2]$ and [Ar] could produce apparent supersaturations in gas concentration. However, as T and S vary very little within the σ_θ 26.0 to 26.4 range (Fig. 3), horizontal mixing could not have produced this effect.

Alternatively, NH_4^+ produced during denitrification and NO_3^- from the water column may have been used to form microbial biomass as ODZs are often observed to have deep particle maxima. This explanation could explain the lack of evidence of an NH_4^+ source for biogenic N_2, especially if the newly produced microbial biomass was N-rich as compared with the organic matter sinking down from the surface. However, to account for the rest of the missing biogenic N_2 through NO_3^- uptake, more organic matter would need to be produced than consumed. Emphasizing that we can account for up to 88% of $NO_3^- + NO_2^-$ removal with respect to the production of biogenic N_2 (Fig. 6d), we have no satisfactory explanation for the missing 12%.

There have been numerous modern studies of ODZ N transformation processes using bottle-enclosed ^{15}N tracer experiments often coupled with molecular characterization of microbial populations. They have shown ODZs to be much more diverse with respect to microbial N pathways than first envisioned calling for dominant roles for anammox and nitrite oxidation. Far fewer have investigated the biogeochemical implications of these findings doing a "reality check" using environmental observations. Notably Chang, Devol, and Emerson (2010, 2012) found approximate equivalence between biogenic N_2 and nitrate deficits for stations within the ODZ of the eastern tropical North Pacific and Arabian Sea. Though in the ETSP (Eastern Tropical South Pacific) and in an eddy hot-spot setting, our results indicate possible general deviation from Richards's stoichiometry with respect to NO_3^- removal and biogenic N_2 production. These findings suggest caution in how biogeochemical models of ODZ are constructed based on the results of tracer-rate studies and stoichiometric assumptions. Given that the presence of a diverse N transforming microbial community in ODZs is irrefutable, it follows that there remain large knowledge gaps in explaining the net biogeochemical changes that result from its activity.

Acknowledgments. Data for this article are available on the Data Management Portal for Kiel Marine Sciences hosted at GEOMAR (M90 and M91 cruises): https://portal.geomar.de/. This work was supported by the Deutsche Forschungsgemeinschaft project SFB 754 (www.sfb754.de), SOPRANII (grant no. FKZ03F0611A; http://www.sopran.pangaea.de), National Science Foundation grants OCE 0851092 and OCE 1154741 to MAA, and an Natural Sciences and Engineering Research Council of Canada postdoctoral fellowship to AB. We would like to thank the captain and crew of R/V *Meteor* during the M90 and M91 cruises, and Net Charoenpong, Martin Frank, Tina Baustian, Martina Lohmann, Janett Voigt, Kristin Doering, Patrick Daniel, Daniel Kiefhaber, Avi Bernales, and Violeta Leon for their help during sampling and/or sample analysis. We also appreciate the support and comments from Hermann Bange and Lothar Stramma. We thank the authorities of Peru for the permission to work in their territorial waters. MAA especially thanks James J. McCarthy for his mentorship and friendship.

REFERENCES

Altabet, M. A. 2007. Constraints on oceanic N balance/imbalance from sedimentary ^{15}N records. Biogeosci., *4*, 75–86. doi: 10.5194/bg-4-75-2007

Altabet, M. A., and J. J. McCarthy. 1985. Temporal and spatial variations in the natural abundance of ^{15}N in PON from a warm-core ring. Deep-Sea Res., Part A, *32*, 755–772. doi: 10.1016/0198-0149(85)90113-X

Altabet, M. A., E. Ryabenko, L. Stramma, D. W. R. Wallace, M. Frank, P. Grasse, and G. Lavik. 2012. An eddy-stimulated hotspot for fixed nitrogen-loss from the Peru oxygen minimum zone. Biogeosci., *9*, 4897–4908. doi: 10.5194/bg-9-4897-2012

Arévalo-Martínez, D. L., A. Kock, C. R. Löscher, R. A. Schmitz, L. Stramma, and H. W. Bange. 2016. Influence of mesoscale eddies on the distribution of nitrous oxide in the eastern tropical South Pacific. Biogeosci., *13*, 1105–1118. doi: 10.5194/bg-13-1105-2016

Babbin, A. R., R. G. Keil, A. H. Devol, and B. B. Ward. 2014. Organic matter stoichiometry, flux, and oxygen control nitrogen loss in the ocean. Science, *344*, 406–408. doi: 10.1126/science.1248364

Bourbonnais, A., M. A. Altabet, C. N. Charoenpong, J. Larkum, H. Hu, H. W. Bange, and L. Stramma. 2015. N-loss isotope effects in the Peru oxygen minimum zone studied using a mesoscale eddy as a natural tracer experiment. Global Biogeochem. Cycles, *29*, 793–811. doi: 10.1002/2014GB005001

Brandes, J. A., A. H. Devol, T. Yoshinari, D. A. Jayakumar, and S. W. A. Naqvi. 1998. Isotopic composition of nitrate in the central Arabian Sea and eastern tropical North Pacific: A tracer for mixing and nitrogen cycles. Limnol. Oceanogr., *43*, 1680–1689. doi:10.4319/lo.1998.43.7.1680

Bristow, L. A., C. M. Callbeck, M. Larsen, M. A. Altabet, J. Dekaezemacker, M. Forth, M. Gauns, et al. 2017. N_2 production rates limited by nitrite availability in the Bay of Bengal oxygen minimum zone. Nat. Geosci., *10*, 24–29. doi: 10.1038/ngeo2847

Callbeck, C. M., G. Lavik, L. Stramma, M. M. M. Kuypers, and L. A. Bristow. 2017. Enhanced nitrogen loss by eddy-induced vertical transport in the offshore Peruvian oxygen minimum zone. PLoS One, *12*, e0170059. doi: 10.1371/journal.pone.0170059

Casciotti, K. L., J. K. Böhlke, M. R. McIlvin, S. J. Mroczkowski, and J. E. Hannon. 2007. Oxygen isotopes in nitrite: Analysis, calibration, and equilibration. Anal. Chem., *79*, 2427–2436. doi: 10.1021/ac061598h

Casciotti, K. L., C. Buchwald, and M. McIlvin. 2013. Implications of nitrate and nitrite isotopic measurements for the mechanisms of nitrogen cycling in the Peru oxygen deficient zone. Deep-Sea Res., Part I, *80*, 78–93. doi: 10.1016/j.dsr.2013.05.017

Chaigneau, A., A. Gizolme, and C. Grados. 2008. Mesoscale eddies off Peru in altimeter records: Identification algorithms and eddy spatio-temporal patterns. Prog. Oceanogr., *79*, 106–119. doi: 10.1016/j.pocean.2008.10.013

Chang, B. X., A. H. Devol, and S. R. Emerson. 2010. Denitrification and the nitrogen gas excess in the eastern tropical South Pacific oxygen deficient zone. Deep-Sea Res., Part I, *57*, 1092–1101. doi: 10.1016/j.dsr.2010.05.009

Chang, B. X., A. H. Devol, and S. R. Emerson. 2012. Fixed nitrogen loss from the eastern tropical North Pacific and Arabian Sea oxygen deficient zones determined from measurements of N_2:Ar. Global Biogeochem. Cycles, *26*, GB3030, doi: 10.1029/2011GB004207

Charoenpong, C. N., L. A. Bristow, and M. A. Altabet. 2014. A continuous flow isotope ratio mass spectrometry method for high precision determination of dissolved gas ratios and isotopic composition. Limnol. Oceanogr.: Methods, *12*, 323–337. doi: 10.4319/lom.2014.12.323

Codispoti, L. A., and J. P. Christensen. 1985. Nitrification, denitrification and nitrous oxide cycling in the eastern tropical South Pacific Ocean. Mar. Chem., *16*, 277–300. doi: 10.1016/0304-4203(85)90051-9

Codispoti, L. A., and T. T. Packard. 1980. Denitrification rates in the eastern tropical South Pacific. J. Mar. Res., *38*, 453–477.

Cornejo D'Ottone, M., L. Bravo, M. Ramos, O. Pizarro, J. Karstensen, M. Gallegos, M. Correa-Ramirez, N. Silva, L. Farias, and L. Karp-Boss. 2016. Biogeochemical characteristics of a long-lived anticyclonic eddy in the eastern South Pacific Ocean. Biogeosci., *13*, 2971–2979. doi: 10.5194/bg-13-2971-2016, 2016

Dalsgaard, T., F. J. Stewart, B. Thamdrup, L. De Brabandere, N. P. Revsbech, O. Ulloa, D. E. Canfield, and E. F. DeLong. 2014. Oxygen at nanomolar levels reversibly suppresses process rates and gene expression in anammox and denitrification in the oxygen minimum zone off northern Chile. mBio, *5*, 01966-14. doi: 10.1128–mBio.01966-14

Dalsgaard, T., B. Thamdrup, and D. E. Canfield. 2005. Anaerobic ammonium oxidation (anammox) in the marine environment. Res. Microbiol., *156*, 457–464. doi: 10.1016/j.resmic.2005.01.011

Dalsgaard, T., B. Thamdrup, L. Farías, and N. P. Revsbech. 2012. Anammox and denitrification in the oxygen minimum zone of the eastern South Pacific. Limnol. Oceanogr., *57*, 1331–1346. doi: 10.4319/lo.2012.57.5.1331

Falkowski, P. G., D. Zieman, Z. Kolber, and P. K. Bienfang. 1991. Role of eddy pumping in enhancing primary production in the ocean. Nature, *352*, 55–58. doi: 10.1038/352055a0

Granger, J., D. M. Sigman, M. F. Lehmann, and P. D. Tortell. 2008. Nitrogen and oxygen isotope fractionation during dissimilatory nitrate reduction by denitrifying bacteria. Limnol. Oceanogr., *53*, 2533–2545. doi: 10.4319/lo.2008.53.6.2533

Granger, J. and D. M. Sigman. 2009. Removal of nitrite with sulfamic acid for nitrate N and O isotope analysis with the denitrifier method. Rapid Commun. Mass Spectrom. 23: 3753–3762. doi: 10.1002/rcm.4307

Gruber, N., and J. L. Sarmiento. 1997. Global patterns of marine nitrogen fixation and denitrification. Global Biogeochem. Cycles, *11*, 235–266. doi: 10.1029/97GB00077

Hamersley, M. R., G. Lavik, and D. Woebken. 2007. Anaerobic ammonium oxidation in the Peruvian oxygen minimum zone. Limnol. Oceanogr., *52*, 923–933. doi: 10.4319/lo.2007.52.3.0923

Hamme, R. C., and S. R. Emerson. 2002. Mechanisms controlling the global oceanic distribution of the inert gases argon, nitrogen and neon. Geophys. Res. Lett., *29*, 2120. doi: 10.1029/2002GL015273

Horak, R. E. A., W. Ruef, B. B. Ward, and A. H. Devol. 2016. Expansion of denitrification and anoxia in the eastern tropical North Pacific from 1972 to 2012. Geophys. Res. Lett., *43*, 5252–5260, doi: 10.1002/2016GL068871

Hu, H., A. Bourbonnais, J. Larkum, H. W. Bange, and M. A. Altabet. 2016. Nitrogen cycling in shallow low oxygen coastal waters off Peru from nitrite and nitrate nitrogen and oxygen isotopes. Biogeosci., *13*, 1453–1468. doi: 10.5194/bg-13-1453-2016

Kalvelage, T., G. Lavik, P. Lam, S. Contreras, L. Arteaga, C. R. Löscher, A. Oschlies, A. Paulmier, L. Stramma, and M. M. M. Kuypers. 2013. Nitrogen cycling driven by organic matter export in the South Pacific oxygen minimum zone. Nat. Geosci., *6*, 228–234. doi: 10.1038/ngeo1739

Keeling, R. F., and H. E. Garcia. 2002. The change in oceanic O_2 inventory associated with recent global warming. Proc. Natl. Acad. Sci. U. S. A., *99*, 7848–7853. doi: 10.1073/pnas.122154899

Lam, P., and M. M. M. Kuypers. 2011. Microbial nitrogen cycling processes in oxygen minimum zones. Annu. Rev. Mar. Sci., *3*, 317–345. doi: 10.1146/annurev-marine-120709-142814

Lam, P., G. Lavik, M. M. Jensen, J. van de Vossenberg, M. Schmid, D. Woebken, D. Gutierrez, R. Amann, M. S. M. Jetten, and M. M. M. Kuypers. 2009. Revising the nitrogen cycle in the Peruvian oxygen minimum zone. Proc. Natl. Acad. Sci. U. S. A., *106*, 4752–4757. doi: 10.1073/pnas.0812444106

Martin, J. H., G. A. Knauer, D. M. Karl, and W. W. Broenkow. 1987. VERTEX: Carbon cycling in the northeast Pacific. Deep-Sea Res., Part A, *34*, 267–285. doi: 10.1016/0198-0149(87)90086-0

McGillicuddy, D. J., Jr., L. A. Anderson, N. R. Bates, T. Bibby, K. O. Buesseler, C. A. Carlson, C. S. Davis, et al. 2007. Eddy/wind interactions stimulate extraordinary mid-ocean plankton blooms. Science, *316*, 1021–1026. doi: 10.1126/science.1136256

McGillicuddy, D. J., Jr., A. R. Robinson, D. A. Siegel, H. W. Jannasch, R. Johnson, T. D. Dickey, J. D. McNeil, A. F. Michaels, and A. H. Knap. 1998. Influence of mesoscale eddies on new production in the Sargasso Sea. Nature, *394*, 263–266. doi: 10.1038/28367

McIlvin, M. R., and M. A. Altabet. 2005. Chemical conversion of nitrate and nitrite to nitrous oxide for nitrogen and oxygen isotopic analysis in freshwater and seawater. Anal. Chem., *77*, 5589–5595. doi: 10.1021/ac050528s

Oschlies, A., and V. Garçon. 1998. Eddy-induced enhancement of primary production in a model of the North Atlantic Ocean. Nature, *394*, 266–269. doi: 10.1038/28373

Redfield, A. 1934. On the proportions of organic derivatives in seawater and their relation to the composition of plankton, *in* James Johnstone Memorial Volume, R. J. Daniel, ed. Liverpool, UK: Liverpool University Press, 176–192.

Revsbech, N. P., L. H. Larsen, J. Gundersen, T. Dalsgaard, O. Ulloa, and B. Thamdrup. 2009. Determination of ultra-low oxygen concentrations in oxygen minimum zones by the STOX sensor. Limnol. Oceanogr.: Methods, *7*, 371–381. doi: 10.4319/lom.2009.7.371

Richards, F. A. 1965. Anoxic basins and fjords, *in* Chemical Oceanography, J. P. Riley and G. Skirrow, eds. London: Academic Press, 611–645.

Ryabenko, E., A. Kock, H. W. Bange, M. A. Altabet, and D. W. R. Wallace. 2012. Contrasting biogeochemistry of nitrogen in the Atlantic and Pacific oxygen minimum zones. Biogeosci., *9*, 203–215. doi: 10.5194/bg-9-203-2012

Stramma L., H. W. Bange, R. Czeschel, A. Lorenzo, and M. Frank. 2013. On the role of mesoscale eddies for the biological productivity and biogeochemistry in the eastern tropical Pacific Ocean off Peru. Biogeosci., *10*, 7293–7306. doi: 10.5194/bg-10-7293-2013

Stramma, L., G. C. Johnson, J. Sprintall, and W. Mohrholz. 2008. Expanding oxygen-minimum zones in the tropical oceans. Science, *320*, 655–658. doi: 10.1126/science.1153847

Stramma, L., G. C. Johnson, E. Firing, and S. Schmidtko. 2010. Eastern Pacific oxygen minimum zones: Supply paths and multidecadal changes. J. Geophys. Res., *115*, C09011, doi: 10.1029/2009JC005976

Stramma, L., M. Visbeck, P. Brandt, T. Tanhua, and D. Wallace. 2009. Deoxygenation in the oxygen minimum zone of the eastern tropical North Atlantic. Geophys. Res. Lett., *36*, L20607. doi: 10.1029/2009GL039593

Stramma, L., G.C Johnson, E. Firing, and S. Schmidtko. 2010. Eastern Pacific oxygen minimum zones: Supply paths and multidecadal changes. J. Geophys. Res., *115*, C09011, doi: 10.1029/2009JC005976

Thamdrup, B., T. Dalsgaard, and N. P. Revsbech. 2012. Widespread functional anoxia in the oxygen minimum zone of the eastern South Pacific. Deep-Sea Res., Part I, *65*, 36–45. doi: 10.1016/j.dsr.2012.03.001

Voss, M., J. W. Dippner, and J. Montoya. 2001. Nitrogen isotope patterns in the oxygen-deficient waters of the eastern tropical North Pacific Ocean. Deep-Sea Res., Part I, *48*, 1905–1921. doi: 10.1016/S0967-0637(00)00110-2

Ward, B. B., A. H. Devol, J. J. Rich, A. Chaigneau, S. E. Bulow, H. Naik, A. Pratihary, and A. Jayakumar. 2009. Denitrification as the dominant nitrogen loss process in the Arabian Sea. Nature, *461*, 78–81. doi: 10.1038/nature08276

Ward, B. B., C. B. Tuit, A. Jayakumar, J. J. Rich, J. Moffett, and S. W. A. Naqvi. 2008. Organic carbon, and not copper, controls denitrification in oxygen minimum zones of the ocean. Deep-Sea Res., Part I, *55*, 1672–1683. doi: 10.1016/j.dsr.2008.07.005

Yang, S., N. Gruber, M. C. Long, and M. Vogt. 2017. ENSO driven variability of denitrification and suboxia in the eastern tropical Pacific Ocean. Global Biogeochem. Cycles, *31*, 1470–1487. doi: 10.1002/2016GB005596

Received: *30 April 2019*; revised: *1 July 2019*.